THE ASTROPHYSICAL JOURNAL, 406:L43–L46, 1993 April 1

THE EVOLUTION OF BRIGHT, OPTICALLY SELECTED QSOs

PAUL C. HEWETT
Institute of Astronomy, Madingley Road, Cambridge, CB3 0HA, UK
AND
CRAIG B. FOLTZ AND FREDERIC H. CHAFFEE
Multiple Mirror Telescope Observatory, University of Arizona, Tucson, AZ 85721
Received 1992 July 22; accepted 1993 January 14

ABSTRACT

We analyze 1049 QSOs and AGNs from the Large Bright QSO Survey to produce new constraints on the shape and evolutionary behavior of the bright end of the QSO luminosity function. The data represent more than an order of magnitude improvement for redshifts $0.2 < z < 3$, and absolute magnitudes corresponding to apparent magnitudes $16.5 < m_{B_J} < 18.85$. The results are poorly described by the predictions of a model in which a two power-law luminosity function of constant shape evolves strongly until redshift $z \sim 2$, in such a way as to mimic the effect of pure-luminosity evolution.

In the Large Bright QSO Survey sample the shape of the luminosity function changes systematically as a function of redshift, becoming steeper at larger redshifts. Compared to current models, the rate of evolution is less rapid over the redshift range $0.2 < z < 2$, but continues, at a significantly reduced rate, until at least redshift $z \sim 3$. A significant revision of the presently accepted model for the evolution of the QSO population is indicated.

Subject headings: cosmology: observations — quasars: general

1. INTRODUCTION

The form and evolution, as a function of look-back time, of the QSO luminosity function (QLF) provide important constraints on the formation processes and lifetimes of QSOs (e.g., Cavaliere & Padovani 1989; Haehnelt & Rees 1993). The normalization and form of the QLF at redshifts $0.5 \lesssim z \lesssim 3$ for absolute magnitudes corresponding to apparent magnitudes $19.5 \lesssim m_B \lesssim 22.0$ are relatively well established (Boyle et al. 1990, Boyle 1991). Brighter than apparent magnitudes $m_B \sim 19$, the situation is less satisfactory; for magnitudes $m_B \lesssim 16$, the Palomar-Green survey (Schmidt & Green 1983) provides the only large sample of QSOs, while at intermediate magnitudes, $16.5 \lesssim m_B \lesssim 19$, data have been confined to a few tens of QSOs (Hartwick & Schade 1990; Boyle 1991, Table 2; Table 1).

At redshifts $z \lesssim 2$, a surprisingly simple "standard picture" has emerged from the analysis of existing samples. The shape of the QLF can be well approximated using a two power-law form that is invariant with redshift (Boyle 1991), with a steep bright end $N(L)dL \propto luminosity^{-3.9}$, and a shallower faint end, $N(L)dL \propto luminosity^{-1.5}$. The form of the evolution is also particularly simple, with the characteristic luminosity (L^*) at the break in the QLF, evolving as a function of redshift, $L^*(z) \propto (1+z)^{3.4}$ – the so-called pure luminosity evolution. Above redshift $z = 2$ what little data are available suggest that the normalisation of the QLF is approximately constant over the redshift range $2 < z < 3$. At higher redshifts $3 < z < 5$, substantial samples have now been acquired by Schmidt et al. (1991), Irwin, McMahon, & Hazard (1991), and Warren, Hewett, & Osmer (1991) and quantitative results from these samples are expected soon. Reviews of the survey techniques and our present knowledge of the QLF can be found in Hartwick & Schade (1990), Warren & Hewett (1990), and Boyle (1991). In this *Letter* we present an analysis of 1049 QSOs and AGNs from the Large Bright QSO Survey (LBQS). The results suggest that a considerable revision of the standard picture is required.

2. LARGE BRIGHT QSO SURVEY

Spectra, redshifts, and magnitudes for the Large Bright QSO Survey (LBQS) QSOs are given in a series of five papers (Morris et al. 1991 and references therein). A sixth paper (Hewett, Foltz, & Chaffee 1993) will provide details of ~1052 objects with redshifts $0.2 \leq z \leq 3.4$. This sample consists of the published QSOs, and AGNs with broad emission lines, excluding five objects which fall outside the boundaries of the final survey area (QSOs 1212+1535, 1230+1440, 1241+1639, 1244+0947, and 1245+1038 in Table II of Foltz et al. 1987), together with seven objects that have been spectroscopically confirmed as QSOs since Morris et al. The latter group have apparent magnitudes and redshifts (m_{B_J}, z): (18.6, 0.26), (16.5, 0.40), (17.0, 0.66), (16.7, 0.67), (17.9, 1.27), (18.2, 1.52) and (18.5, 1.71). Minor revisions to the magnitude scale ($\lesssim$0.1 mag) in four fields and the correct assignment of a redshift of $z = 1.41$ to object 1326+0206 are also included. The small revisions to the magnitude scale for the four Virgo fields (Hewett et al. 1991) make no material difference to the results reported here.

The analysis described here is based on 1049 QSOs and AGNs, apparent magnitudes $16.5 \leq m_{B_J} \leq 18.85$, redshifts $0.2 \leq z \leq 3.4$. A precise "effective area" has been calculated as a function of apparent magnitude. Table 1 lists the apparent magnitude, m_{B_J}, and the associated effective area, in square degrees, covered by the LBQS. The number magnitude relations for the entire sample, and also for QSOs in the redshift interval $0.2 \leq z \leq 2.2$ and absolute magnitudes $M_{B_J} \leq -23$, are in excellent agreement with the results of Goldschmidt et al. (1992) and compilations of data from the literature (e.g., Fig. 1 of Goldschmidt et al.). A direct comparison of LBQS apparent magnitudes of QSOs and stars in the Boyle et al. (1990) catalog (more than half of the Boyle et al. QSOs lie within the

TABLE 1

LBQS EFFECTIVE SURVEY AREA

Limiting Magnitude (m_{B_J})	Effective Area (square degrees)
18.41	453.8
18.46	431.4
18.50	405.5
18.55	350.9
18.62	299.8
18.64	246.1
18.67	223.2
18.68	201.1
18.74	174.3
18.75	149.1
18.76	129.0
18.77	101.2
18.80	48.5
18.85	21.5

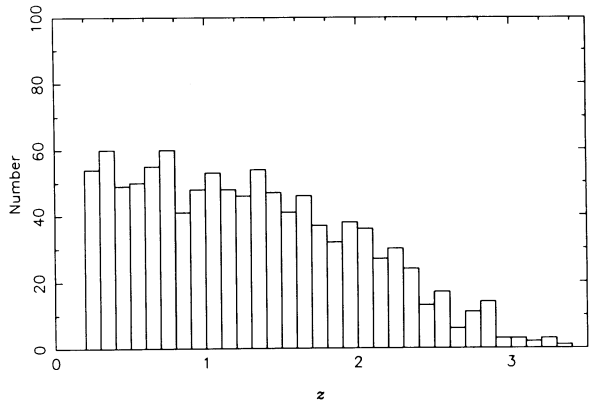

FIG. 1.—Number-redshift histogram for the 1049 LBQS QSOs and AGNs used in the derivation of the QSO luminosity function.

LBQS fields), shows no evidence of significant differences in zero point for magnitudes $m_{B_J} < 19$.

The k-corrections were calculated for the B_J passband from the spectrum of Cristiani & Vio (1990) modified below 1250 Å to include the effects of absorption by intervening hydrogen clouds according to the prescription of Møller & Warren (1991). The results are not sensitive to the details of the k-corrections. Throughout this *Letter* we have employed k-corrections for the B_J passband and a cosmology with Hubble Constant $H_0 = 50$ km s^{-1} Mpc^{-1}, deceleration parameter $q_0 = 0.5$ and cosmological constant $\Lambda = 0$. Using this model, 997 of the objects have absolute magnitudes $M_{B_J} \leq -23$, and the remaining 52 objects have absolute magnitudes representative of the brightest Seyfert galaxies, $-23 < M_{B_J} < -21.7$, all of which lie in the redshift interval $0.2 < z < 0.4$. Exclusion of the objects with $M_{B_J} > -23$ would simply truncate the data at brighter absolute magnitudes in the redshift shell, $0.2 \leq z \leq 0.5$.

The calculation of the probability of including a QSO in the LBQS as a function of redshift, absolute magnitude and spectral energy distribution (SED) has yet to be completed. However, there is a significant corpus of evidence to support the claim that the probability of including a QSO is at least as great or greater than that for other optically based surveys, and furthermore, that the probability of including a QSO does not vary significantly as a function of redshift, absolute magnitude, or QSO SED: (1) the redshift histogram, Figure 1, is smooth. Any significant variation in the probability of inclusion as a function of redshift would have to be anticorrelated with variations in the intrinsic $n(z)$ relation so as to give the smooth function observed, (2) the number magnitude counts for the LBQS are in good agreement with recent determinations (e.g., Goldschmidt et al. 1992), (3) the spectra investigated in the LBQS include 160 QSOs listed in the Hewitt & Burbidge catalog (1987, 1989) of which 159 were recovered independently, (4) the range of QSO SEDs included in the LBQS is at least as extensive as in any other optically based survey, and significantly more extended than in most (e.g., Francis et al. 1992), and (5) only 11 of the >2000 objects observed spectroscopically remain to be positively identified, i.e., the maximum possible fractional incompleteness from this source is 1% (11/1049 spectra).

3. RESULTS

The data have been analysed in a series of redshift shells using the $1/V_{\rm access}$ estimator (eq. [1] of Felton 1976). Earlier studies of optically selected QSO samples have displayed results in differential form, employing bins covering a significant interval in absolute magnitude ($\Delta M = 0.5$–1.0). This leads to an undesirable level of smoothing at all absolute magnitudes, and at the extremes of the absolute magnitude range the apparent magnitude limits, which define the sample, involve a complicated weighting as a function of redshift. As a result it is not clear what the appropriate "mean" absolute magnitude for bins at the bright and faint end should be. This difficulty, together with the undesirable smoothing at all absolute magnitudes is exacerbated by the steep dependence of the space density on absolute magnitude.

Displaying the results in cumulative form, as employed frequently in the discussion of X-ray–selected samples (e.g., Marshall 1991) circumvents the requirement for binning and the problems induced by incompleteness at the extremes of the absolute magnitude range. The cumulative representation also possesses the advantage of displaying the contribution to the space density made by each individual QSO (we are grateful to Mike Irwin for pointing out the substantial advantages of adopting this representation). Figure 2*a* shows the cumulative space density calculated using the LBQS sample divided into seven redshift shells, with boundaries 0.2–0.5, 0.5–1.0, 1.0–1.5, 1.5–2.0, 2.0–2.5, 2.5–3.0, and 3.0–3.4. The line styles have been alternated to aid the identification of the data for each shell. The number of QSOs contributing to the space density estimates of Figure 2*a* represent an increase of a factor ~ 20 over existing samples covering the same apparent magnitude range.

Figure 2*b* shows the cumulative space density calculated for the four redshift shells 0.2–0.5, 0.5–1.0, 1.0–1.5, and 1.5–2.0, together with the equivalent cumulative space densities derived from the two power-law QLF models:

$$\phi(M_{B_J}, z)dM_{B_J}dz = \phi^*\{10^{0.4[M_{B_J} - M_{B_J}(z)](\alpha+1)} + 10^{0.4[M_{B_J} - M_{B_J}(z)](\beta+1)}\}^{-1}dM_{B_J}dz$$

with a pure-luminosity evolution of the characteristic magnitude, $M_{B_J}(z)$:

$$M_{B_J}(z) = M^*_{B_J} - 2.5k_L \log(1+z) \quad z < z_{\rm max}$$

$$M_{B_J}(z) = M_{B_J}(z_{\rm max}) \quad z > z_{\rm max}$$

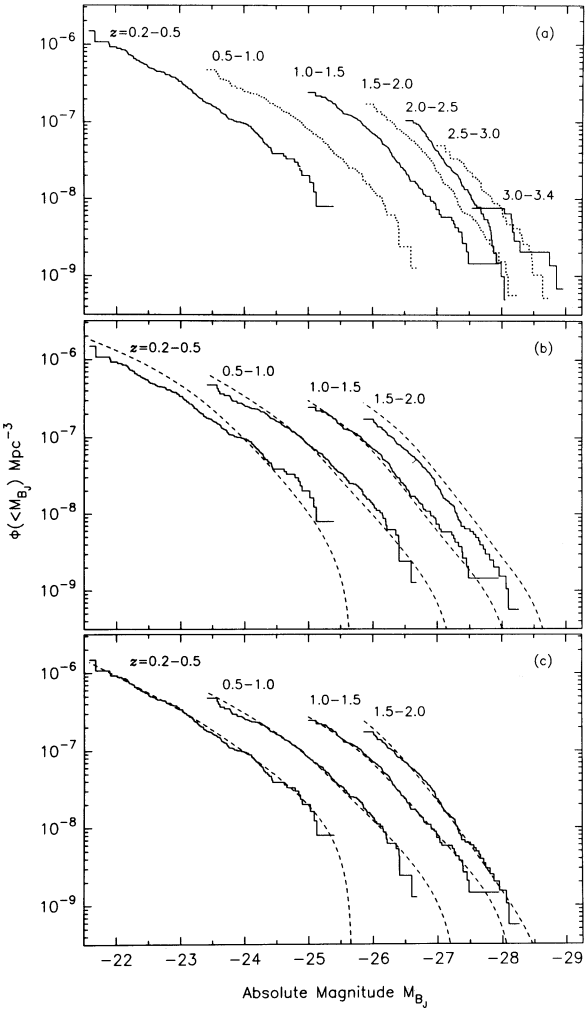

FIG. 2.—(*a*) The cumulative space density of QSOs, $\Phi(< M_{B_J}, \mathrm{Mpc}^{-3})$, brighter than absolute magnitude, M_{B_J}, derived from the LBQS sample in seven redshift shells: $z = 0.2$–0.5, $z = 0.5$–1.0, $z = 1.0$–1.5, $z = 1.5$–2.0, $z = 2.0$–2.5, $z = 2.5$–3.0, $z = 3.0$–3.4. (*b*) LBQS data for the four redshift shells covering 0.2–2.0: *solid lines*, as in (*a*), together with the predictions of the two power-law model undergoing pure luminosity evolution: *dashed lines*. Parameter values taken from Boule (1991). (*c*) LBQS data for the four redshift shells covering 0.2–2.0: *solid lines*, as in (*a*), together with the predictions of the two power-law model after ad hoc adjustments (see text) to the power-law slopes specifying the shape of the QLF and the redshift at which the pure-luminosity evolution ceases.

with numerical values from Boyle (1991): $\phi^* = 6.5 \times 10^{-7}$ mag^{-1} Mpc^{-3}, $\alpha = -3.9$, $\beta = -1.5$, $M^*_{B_J} = -22.5$, $k_L = 3.45$, $z_{\mathrm{max}} = 1.9$.

In a sample limited by apparent magnitude, the fraction of each shell that is accessible changes as a function of absolute magnitude in such a way that the data at fainter absolute magnitudes is weighted to lower redshifts. Only in the case where the QLF does not evolve across the shell will the space density as a function of absolute magnitude calculated within the shell by this method represent the true QLF. In the presence of evolution, the space density derived depends both on the form of the evolution across the shell and the shape of the QLF. For an increase in space density as a function of increasing redshift, as is the case for QSOs with redshifts $z \lesssim 2$, the space density derived will exhibit a flattening toward fainter absolute magnitudes. The bright absolute magnitude limit, M_{far}, for a shell corresponds to the absolute magnitude of a QSO with apparent magnitude $m_{B_J} = 16.5$ at the redshift of the far edge of the shell. The sample contains no information for brighter absolute magnitudes, and, as a consequence, the cumulative space density shows a steep turndown at bright absolute magnitudes close to this limit. The cumulative space density, $\phi(< M)$, plotted in Figure 2 is defined by

$$\phi(<M) = \int_{M}^{M_{\mathrm{far}}} dM \, \frac{\int_{z_1}^{z_2} \phi(M, z)\Omega(M, z)(dV/dz)dz}{\int_{z_1}^{z_2} \Omega(M, z)(dV/dz)dz}$$

where $\phi(M, z)$, is the differential luminosity function, and $\Omega(M, z)$ the solid angle. The redshift limits, $z_1 z_2$, correspond to the near and far edges of the shell.

The space densities calculated from the Boyle model have been derived using the same procedure. Thus, Figure 2 represents a direct comparison between the data and the predictions of the model.

There is a large systematic difference in the total number of QSOs observed compared to the model prediction. The predicted versus observed number in each shell being (262, 163), (322, 254), (257, 248) and (285, 194) for the four shells in order of increasing redshift. Relative to the model predictions these correspond to deficits of 6.1 σ, 3.8 σ, 0.6 σ and 5.4 σ, respectively. To bring the model and data into agreement requires $\sim$270 QSOs to be added to the LBQS sample. Such an increase would produce a surface density of QSOs in conflict with the best available number magnitude counts, and it is hard to reconcile with the other tests of the efficacy of the selection (§ 2). The space density calculation has been performed restricting the sample to QSOs brighter than apparent magnitude $m_{B_J} = 18.5$ and also to subsamples restricted to objects at last 0.1–0.5 mag brighter than the corresponding magnitude limit in each of the 18 individual LBQS fields. The resulting estimates of the space density are truncated at brighter absolute magnitudes but the shape and normalizations do not change: significant differential incompleteness as a function of apparent magnitude is not responsible for the differences. A deficit of faint objects at low redshifts is evident in the data of Boyle et al., but it has been thought that the presence of underlying galaxies could result in objects eluding the selection criteria of the sample which are based on "stellar" objects exhibiting an ultraviolet excess. The selection of the LBQS candidates includes resolved objects, in order to identify potential gravitational lenses, and the color changes caused by the presence of galaxies at $z > 0.2$ does not preclude the identification of spectra as candidate QSOs. Thus, we believe this deficit, relative to the model prediction, is real.

Inspection of Figure 2*b* also shows systematic differences in the shape of the observed curves and the predictions of the model. The cumulative space density curves appear to steepen with increasing redshift until the $z = 1.5$–2.0 shell where the model and data appear to be in excellent agreement. At lower redshifts the cumulative space density curves exhibit a substantially shallower slope than the model. A Kolmogorov-Smirnov test, applied to the cumulative number of QSOs predicted versus number observed in each shell, as a function of absolute magnitude, produces D_{max} values and associated probabilities of (0.077, 0.286), (0.099, 0.014), (0.086, 0.050), and (0.047, 0.790), respectively. The statistic confirming the apparent differences between data and model in the redshift shells $z = 0.5$–1.0 and $z = 1.0$–1.5, and consistency for the shell $z = 1.5$–2.0. The

excess number of bright QSOs, relative to the model, in the lowest redshift shell ($z = 0.2$–0.5) is too small to be formally significant. As applied, the Kolmogorov-Smirnov test gives an extremely conservative estimate of the significance of the differences between model and data as no attempt has been made to perform a statistical test that highlights the systematic trends evident in Figure 2*b*. Furthermore, no account of the substantial difference in normalization is taken.

At redshifts $z > 2$ there is evidence for continued evolution over the range $2 \lesssim z \lesssim 3$. For a QLF of constant shape, as specified by Boyle (1991), evolving according to the pure-luminosity evolution description, then the data can be represented by the characteristic luminosity changing as $L^*(z) \propto (1 + z)^{1.5}$. At redshifts $z > 3$ there are too few QSOs to constrain any model effectively, although the data are consistent with a constant space density for redshifts $z = 3.0$–3.4.

4. DISCUSSION

Perhaps the most striking feature of the LBQS data is the systematic change in shape of the cumulative space density as a function of redshift. To set quantitative limits on the shape of the QLF as a function of redshift and to determine the rate and form of evolution will require extensive analysis, together with additional data to constrain the behavior at fainter absolute magnitudes. However, to illustrate the size of the changes to the existing model implied by the new LBQS analysis, ad hoc modifications to the parameters of the two power-law representation of the QLF and the redshift at which the pure-luminosity evolution ceases, have been made. The LBQS data are shown again in Figure 2*c*. In the model the value of the evolution parameter, k_L, has been retained, but for the $z = 0.2$–0.5 shell the QLF normalization has been reduced to $\phi^* = 4.0 \times 10^{-7}$ mag^{-1} Mpc^{-3}, the bright end slope set to $\alpha = -2.75$, and faint end slope $\beta = -2.0$. The two redshift shells, 0.5–1.0 and 1.0–1.5, both have QLF slopes, $\alpha = -3.6$, $\beta = -1.5$ and $\phi^* = 5.5 \times 10^{-7}$ mag^{-1} Mpc^{-3}. The shell 1.5–2.0 retains the normalization and shape of the QLF from Boyle but the evolution is halted at $z = 1.65$, cf. $z = 1.9$ from Boyle. A comparison of the revised model with the data in the four shells using a Kolmogorov-Smirnov statistic confirm they are consistent. Thus, the LBQS data is consistent with a model in which the shape of the QLF steepens significantly as a function of redshift. However, the ad hoc changes are only one example of a wide range of possible modifications to the shape of the QLF and the form of the evolution as a function of redshift that produce results consistent with the data.

The analysis of the LBQS demonstrates: (1) the space density of luminous QSOs at redshift $z \lesssim 1$ is larger than that predicted by the model (in agreement with Goldschmidt et al. 1992), (2) at redshifts ~ 1.5, the rate of evolution must depart from the very fast, $L^*(z) \propto (1 + z)^{3.4}$, derived by Boyle (1991) and others, and (3) there is evidence for continued evolution over the range $2 \lesssim z \lesssim 3$—retaining the pure-luminosity evolution parameterization, then $L^*(z) \propto (1 + z)^{1.5}$. These results have important implications for the theoretical problem of why the space density of QSOs undergoes such a dramatic change with cosmic time (e.g., Fig. 2 of Schmidt et al. 1991). Increasing the space density at low redshift, decreasing the rate at which the evolution proceeds but increasing the redshift out to which the evolution extends, has the effect of broadening the half-width of the peak in space density. This is equivalent to the space density of QSOs changing more slowly with cosmic time, a factor that can only make the theoretical problem of explaining the underlying physics behind the peak more tractable. How the QLF managed to retain an invariant shape while the space density changed by two orders of magnitude, or equivalently, the characteristic luminosity changed by a factor ~ 50, has never been clear. The LBQS results indicate that this puzzle may no longer be a problem. Gravitational lensing has often been proposed as a method for generating the steep portion of the QLF. The results reported here conflict with the simplest version of this hypothesis, in which, for an intrinsic QLF shape independent of redshift, the bright end of the QLF observed is expected to flatten with increasing redshift.

The LBQS is supported by National Science Foundation Grant Nos. AST-90-01181 and 90-05117. The LBQS would not have been possible without the active support of the United Kingdom Schmidt Telescope Unit and the staff of the Automated Plate Measuring facility. The computations presented in this paper were undertaken on the SERC STARLINK Network. We thank B. Boyle, M. Irwin, L. Miller, and especially S. Warren for clarifying our thoughts. S. Warren kindly made available the *k*-corrections for the B_J passband. P. C. H. is particularly grateful to Mike Irwin for his patience during the generation of this paper.

REFERENCES

Boyle, B. J. 1991, in Proc. Texas/ESO-CERN Symposium on Relativistic Astrophysics, Cosmology, Fundamental Physics, ed. J. D. Barrow, L. Mestel, & P. A. Thomas 14
Boyle, B. J., Fong, R., Shanks, T., & Peterson, B. 1990, MNRAS, 243, 1
Cavaliere, A., & Padovani, P. 1989, ApJLett, 340, L5
Cristiani, S., & Vio, R. 1990, A&A, 227, 385
Felton, J. E. 1976, ApJ, 207, 700
Foltz, C. B., Chaffee, F. H., Hewett, P. C., MacAlpine, G. M., Turnshek, D. A., Weymann, R. J., & Anderson, S. F. 1987, AJ, 94, 1423
Francis, P. J., Hewett, P. C., Foltz, C. B., & Chaffee, F. H. 1992, ApJ 398, 476
Goldschmidt, P., Miller, L., La Franca, F., & Cristiani, S. 1992, MNRAS, 256, 65p
Haehnelt, M. G. & Rees, M. J. 1993, MNRAS, in press
Hartwick, F. D. A., & Schade, D. 1990, ARA&A, 28, 437
Hewett, P. C., Foltz, C. B., & Chaffee, F. H. 1993, in preparation
Hewett, P. C., Foltz, C. B., Chaffee, F. H., Francis, P. J., Weymann, R. J., Morris, S. L., Anderson, S. F. & MacAlpine, G. M. 1991, AJ, 101, 1121
Hewitt, A., & Burbidge, G. 1987, ApJS, 63, 1
———. 1989, ApJS, 69, 1
Irwin, M. J., McMahon, R. G., & Hazard, C. 1991, in the Space Distribution of Quasars, ed. D. Crampton, ASP Conf. Ser. 21 (San Francisco: ASP), 117
Marshall, H. L. 1991, in The Space Distribution of Quasars, ed. D. Crampton, ASP Conf. Ser. 21 (San Francisco: ASP), 184
Møller, P., & Warren, S. J. 1991, in The Space Distribution of Quasars, ed. D. Crampton, ASP Conf. Ser. 21 (San Francisco: ASP), 96
Morris, S. L., Weymann, R. J., Anderson, S. F., Hewett, P. C., Foltz, C. B., Chaffee, F. H., Francis, P. J., & MacAlpine, G. M. 1991, AJ, 102, 1627
Schmidt, M., & Green, R. F. 1983, ApJ, 269, 352
Schmidt, M., Schneider, D. P., & Gunn, J. E. 1991, in The Space Distribution of Quasars, ed. D. Crampton, ASP Conf. Ser. 21 (San Francisco: ASP), 109
Warren, S. J., & Hewett, P. C. 1990, Rep. Prog. Phys. 54, 243 (Rev. version reprinted in Observational Astrophysics, ed. R. E. White [London: Institute of Physics], 243 [1992])
Warren, S. J., Hewett, P. C., & Osmer, P. S. 1991, in The Space Distribution of Quasars, ed. D. Crampton, ASP Conf. Ser. 21 (San Francisco: ASP), 139